



**HAL**  
open science

# Enhanced Dictionary-Based SAR Amplitude Distribution Estimation and its Validation with Very High Resolution Data

Vladimir Krylov, Gabriele Moser, Sebastiano B. Serpico, Josiane Zerubia

► **To cite this version:**

Vladimir Krylov, Gabriele Moser, Sebastiano B. Serpico, Josiane Zerubia. Enhanced Dictionary-Based SAR Amplitude Distribution Estimation and its Validation with Very High Resolution Data. IEEE Geoscience and Remote Sensing Letters, 2011, 8 (1), pp.148-152. 10.1109/LGRS.2010.2053517 . inria-00503893

**HAL Id: inria-00503893**

**<https://inria.hal.science/inria-00503893>**

Submitted on 3 Feb 2011

**HAL** is a multi-disciplinary open access archive for the deposit and dissemination of scientific research documents, whether they are published or not. The documents may come from teaching and research institutions in France or abroad, or from public or private research centers.

L'archive ouverte pluridisciplinaire **HAL**, est destinée au dépôt et à la diffusion de documents scientifiques de niveau recherche, publiés ou non, émanant des établissements d'enseignement et de recherche français ou étrangers, des laboratoires publics ou privés.

# Enhanced Dictionary-Based SAR Amplitude Distribution Estimation and Its Validation With Very High-Resolution Data

Vladimir A. Krylov, Gabriele Moser, *Member, IEEE*,  
Sebastiano B. Serpico, *Fellow, IEEE*, and Josiane Zerubia, *Fellow, IEEE*

**Abstract**—In this letter, we address the problem of estimating the amplitude probability density function (pdf) of single-channel synthetic aperture radar (SAR) images. A novel flexible method is developed to solve this problem, extending the recently proposed dictionary-based stochastic expectation maximization approach (developed for a medium-resolution SAR) to very high-resolution (VHR) satellite imagery, and enhanced by introduction of a novel procedure for estimating the number of mixture components, that permits to reduce appreciably its computational complexity. The specific interest is the estimation of heterogeneous statistics, and the developed method is validated in the case of the VHR SAR imagery, acquired by the last-generation satellite SAR systems, TerraSAR-X and COSMO-SkyMed. This VHR imagery allows the appreciation of various ground materials resulting in highly mixed distributions, thus posing a difficult estimation problem that has not been addressed so far. We also conduct an experimental study of the extended dictionary of state-of-the-art SAR-specific pdf models and consider the dictionary refinements.

**Index Terms**—Finite mixture models, parametric estimation, probability density function estimation, stochastic expectation maximization (SEM), synthetic aperture radar (SAR) images.

## I. INTRODUCTION

THE ACCURATE modeling of statistical information is a crucial problem in the context of synthetic aperture radar (SAR) image processing and its applications. Specifically, an accurate probability density function (pdf) estimate can effectively improve the performance of SAR image denoising [1] or classification [2]. The very high resolution (VHR) imagery, provided by, for example, the last-generation SAR satellite systems, such as TerraSAR-X and COSMO-SkyMed (COstellation of small Satellites for the Mediterranean basin

Observation), allows the appreciation of various ground materials resulting in highly mixed distributions. The resulting spatial heterogeneity is a critical problem in applications to image classification (the estimation of class-conditional statistics) or filtering (the estimation of local statistics, e.g., in moving-window approaches) [1]. The analysis and modeling of heterogeneous VHR SAR data pose a difficult statistical problem, which, to the best of our knowledge, has not been addressed so far.

Over the years, a number of methods have been proposed for modeling SAR amplitude pdfs. Nonparametric methods, e.g., Parzen window estimator [3] and support vector machines [4], do not assume any specific analytical model for the unknown pdf, thus providing a higher flexibility, although usually involving a manual specification of internal architecture parameters [3]. Parametric methods postulate a given mathematical model for each pdf and formulate the pdf-estimation problem as a parameter estimation problem. Empirical pdf models, including lognormal [1], Weibull [1], Fisher [2], and, recently, the generalized Gamma distribution (GFD) [5], have been reported to model accurately the amplitude SAR images with different heterogeneous surfaces. Several theoretical models, such as Rayleigh [1], Nakagami [1], generalized Gaussian Rayleigh (GGR) [6], symmetric- $\alpha$ -stable generalized Rayleigh ( $S\alpha$ SGR) [7],  $\mathcal{K}$  [8] ( $\mathcal{K}$ -root for amplitudes), and  $\mathcal{G}$  [9], have been derived from specific physical hypotheses for SAR images with different properties. However, several parametric families turned out to be effective only for specific land-cover typologies [1], making the choice of a single optimal SAR amplitude parametric pdf model a hard task, particularly in the case of heterogeneous imagery. To solve this problem, the dictionary-based stochastic expectation maximization (DSEM) approach was developed in [10] for a medium-resolution SAR. It addresses the problem by adopting a finite mixture model (FMM) [11] for the SAR amplitude pdf, i.e., by postulating the unknown amplitude pdf to be a linear combination of parametric components, each corresponding to a specific statistical population.

In this letter, we address the general problem of modeling the statistics of the single-channel SAR amplitude images and, specifically, the VHR SAR. Given the variety of approaches previously mentioned, we extend and enhance the DSEM technique proposed in [10] for a coarser-resolution SAR. We expect the DSEM to be an appropriate tool for this modeling problem, since it is a flexible method, intrinsically modeling the SAR statistics as resulting from mixing several populations, and it is not constrained to a specific choice of a given parametric

Manuscript received March 5, 2010; revised June 10, 2010; accepted June 14, 2010. Date of publication July 26, 2010; date of current version December 27, 2010. The work of V. A. Krylov was supported in part by the French Space Agency (Centre National d'Études Spatiales), by the Poncelet Laboratory, Moscow, and by the Institut National de Recherche en Informatique et en Automatique (INRIA).

V. A. Krylov is with the Department of Mathematical Statistics, Faculty of Computational Mathematics and Cybernetics, Lomonosov Moscow State University, 119991, Moscow, Russia, and also with the Projet Ariana, INRIA/I3S, 06902 Sophia Antipolis, France (e-mail: vkrylov@cs.msu.ru).

G. Moser and S. B. Serpico are with the Department of Biophysical and Electronic Engineering (DIBE), University of Genoa, 16145 Genoa, Italy (e-mail: gabriele.moser@unige.it; sebastiano.serpico@unige.it).

J. Zerubia is with the Projet Ariana, INRIA/I3S, 06902 Sophia Antipolis, France (e-mail: Josiane.Zerubia@sophia.inria.fr).

Digital Object Identifier 10.1109/LGRS.2010.2053517

TABLE I  
PDFS AND MoLC EQUATIONS FOR THE PARAMETRIC PDF FAMILIES IN  $\mathcal{D}$ . HERE,  $\Gamma(\cdot)$  IS THE GAMMA FUNCTION [12],  $K_\alpha(\cdot)$  IS THE  $\alpha$ TH-ORDER MODIFIED BESSEL FUNCTION OF THE SECOND KIND [12],  $J_0(\cdot)$  IS THE ZEROth ORDER BESSEL FUNCTION OF THE FIRST KIND [12],  $\Psi(\cdot)$  IS THE DIGAMMA FUNCTION [12],  $\Psi(\nu, \cdot)$  IS THE  $\nu$ TH-ORDER POLYGAMMA FUNCTION [12], AND  $G_\nu(\cdot)$  DENOTES THE SPECIFIC INTEGRAL FUNCTIONS FOR GGR [6]

| Family |                     | Probability density function  | MoLC equations   |
|--------|---------------------|---|--|
| $f_1$  | Lognormal           | $f_1(r m, \sigma) = \frac{1}{\sigma r \sqrt{2\pi}} \exp\left[-\frac{(\ln r - m)^2}{2\sigma^2}\right]$ , $r > 0$ ,   | $\kappa_1 = m$ , $\kappa_2 = \sigma^2$ .   |
| $f_2$  | Weibull             | $f_2(r \eta, \mu) = \frac{\eta}{\mu^\eta} r^{\eta-1} \exp\left[-\left(\frac{r}{\mu}\right)^\eta\right]$ , $r \geq 0$ ,  | $\kappa_1 = \ln \mu + \eta^{-1}\Psi(1)$ , $\kappa_2 = \eta^{-2}\Psi(1, 1)$ .   |
| $f_3$  | Fisher              | $f_3(r L, M, \mu) = \frac{\Gamma(L+M)}{\Gamma(L)\Gamma(M)} \frac{[ar]^L}{r^{1+ar} L+M}$ , $r > 0$ ,<br>with $a = L/(M\mu)$ ,  | $\kappa_1 = \ln \mu + (\Psi(L) - \ln L) - (\Psi(M) - \ln M)$ ,<br>$\kappa_j = \Psi(j-1, L) + (-1)^j \Psi(j-1, M)$ , $j = 2, 3$ .   |
| $f_4$  | GFD                 | $f_4(r \nu, \kappa, \sigma) = \frac{\nu}{\sigma \Gamma(\kappa)} \left(\frac{r}{\sigma}\right)^{\kappa\nu-1} \exp\left[-\left(\frac{r}{\sigma}\right)^\nu\right]$ , $r \geq 0$ ,   | $\kappa_1 = \Psi(\kappa)/\nu + \ln \sigma$ , $\kappa_j = \Psi(j-1, \kappa)/\nu^j$ , $j = 2, 3$ .   |
| $f_5$  | Nakagami            | $f_5(r L, \lambda) = \frac{2}{\Gamma(L)} (\lambda L)^L r^{2L-1} \exp[-\lambda L r^2]$ , $r \geq 0$ ,  | $2\kappa_1 = \Psi(L) - \ln \lambda L$ , $4\kappa_2 = \Psi(1, L)$ .   |
| $f_6$  | $\mathcal{K}$ -root | $f_6(r L, M, \mu) = \frac{4}{\Gamma(L)\Gamma(M)} [\lambda L M]^{(L+M)/2}$<br>$\times r^{L+M-1} K_{M-L}(2r [\lambda L M]^{1/2})$ , $r \geq 0$ ,  | $2\kappa_1 = \Psi(L) + \Psi(M) - \ln L M \lambda$ ,<br>$2^j \kappa_j = \Psi(j-1, L) + \Psi(j-1, M)$ , $j = 2, 3$ .   |
| $f_7$  | GGR                 | $f_7(r \lambda, \gamma) = \frac{\gamma^2 r}{\lambda^2 \Gamma^2(\lambda)} \int_0^{\pi/2} \exp[-(\gamma r)^{1/\lambda} s(\theta)] d\theta$ , $r \geq 0$ ,<br>with $s(\theta) =  \cos \theta ^{1/\lambda} +  \sin \theta ^{1/\lambda}$ , | $\kappa_1 = \lambda \Psi(2\lambda) - \ln \gamma - \lambda G_1(\lambda) [G_0(\lambda)]^{-1}$ ,<br>$\kappa_2 = \lambda^2 [\Psi(1, 2\lambda) + \frac{G_2(\lambda)}{G_0(\lambda)} - \left(\frac{G_1(\lambda)}{G_0(\lambda)}\right)^2]$ . |
| $f_8$  | S $\alpha$ SGR      | $f_8(r \alpha, \gamma) = r \int_0^{+\infty} \rho \exp[-\gamma \rho^\alpha] J_0(r\rho) d\rho$ , $r \geq 0$ ,   | $\alpha \kappa_1 = (\alpha - 1)\Psi(1) + \ln \gamma 2^\alpha$ , $\kappa_2 = \alpha^{-2}\Psi(1, 1)$ .   |

model allowing to benefit from many of them (dictionary approach). Thus, we extend the earlier DSEM approach to the VHR satellite SAR and enhance it by a novel procedure for estimating the number of mixture components, which enables to reduce appreciably its computational complexity (as much as five times in some cases), resulting in an enhanced DSEM algorithm (EDSEM). We revise the dictionary content with respect to the VHR data by adding the Fisher pdf, which is a particular case of the Snedecor–Fisher distribution and was suggested for a heterogeneous high-resolution (HR) SAR, and the GFD, which is a very flexible empirical model, that includes Weibull and Nakagami as particular cases, and the lognormal as an asymptotic case.

The main novel contribution of this letter is the highly accurate flexible computationally fast pdf-estimation model for the single-channel SAR amplitude images and its validation with the VHR satellite SAR data. We also perform a comparative experimental study of the parametric pdf models in the dictionary (most of the state-of-the-art models), suggesting a refinement of the dictionary for this problem. The scope of the applications where the developed approach can be used includes SAR image equalization, segmentation, and supervised classification.

This letter is organized as follows. In Section II, we propose the EDSEM algorithm. Section III reports the experiments of the developed technique on the VHR satellite SAR images acquired by the TerraSAR-X and COSMO-SkyMed and, on a VHR image, acquired by the RAMSES (Radar Aeroporte Multi-spectral d’Etude des Signatures) sensor. Finally, the conclusions are drawn in Section IV.

## II. METHODOLOGY

To take into account the heterogeneous scenario, when several distinct land-cover typologies are present in the same SAR image, an FMM [11] for the distribution of grey levels is

assumed. An amplitude SAR image is modeled as a set  $\mathcal{I} = \{r_1, \dots, r_N\}$  of independent samples drawn from a mixture pdf with  $K$  components

$$p_r(r) = \sum_{i=1}^K P_i p_i(r), \quad r \geq 0 \quad (1)$$

where  $p_i(r)$  denotes the parametric pdfs and  $\{P_i\}$  represents the mixing proportions:  $\sum_{i=1}^K P_i = 1$ , with  $0 \leq P_i \leq 1$ ,  $i = 1, \dots, K$ . Each component  $p_i(r)$  in (1) is modeled by resorting to a finite dictionary  $\mathcal{D} = \{f_1, \dots, f_8\}$  (see Table I) of eight SAR-specific distinct parametric pdfs  $f_j(r|\theta_j)$  parameterized by  $\theta_j \in A_j$ ,  $j = 1, \dots, 8$ . Dealing with the VHR heterogeneous SAR, we include the Fisher model, suggested for the heterogeneous HR SAR imagery, and the GFD, which is a highly flexible empirical model, that includes lognormal, Weibull, and Nakagami as special cases, into the considered dictionary  $\mathcal{D}$ .

As discussed in [10], considering the variety of estimation approaches for the FMMs, an appropriate choice for this particular estimation problem is the stochastic expectation maximization (SEM) scheme [11]. The SEM was developed as a stochastic modification of the classical expectation maximization (EM) algorithm, involving stochastic sampling on every iteration and demonstrating higher chances of avoiding the local maxima of the likelihood function [11]. The SEM is an iterative estimation procedure dealing with the problem of *data incompleteness*. In case of the FMMs, the complete data are represented by the set  $\{(r_i, s_i), i = 1, \dots, N\}$ , where  $r_i$  denotes the observations (SAR amplitudes) and  $s_i$  represents the missing labels: Given an FMM with  $K$  components,  $s_i \in \{\sigma_1, \sigma_2, \dots, \sigma_K\}$  denotes to which of the  $K$  components the  $i$ th observation belongs.

Instead of adopting the maximum likelihood (ML) estimates as the classical SEM scheme [11] suggests, in the DSEM, the method of log-cumulants (MoLC) [2] for the component parameter estimation is adopted, which has been demonstrated

to be a feasible and effective estimation tool for all the pdfs in  $\mathcal{D}$  [2], [5], [10]. The MoLC has recently been proposed as a parametric pdf-estimation technique suitable for the distributions defined on  $[0, +\infty)$  and has been widely applied in the context of the SAR-specific parametric families for amplitude and intensity data modeling. The MoLC adopts the Mellin transform [12] by analogy to the Laplace transform in a moment generating function [2]. Given a nonnegative random variable  $u$ , the second-kind characteristic function  $\phi_u$  of  $u$  is defined as the Mellin transform [12]  $\mathcal{M}$  of the pdf of  $u$ , i.e.,

$$\phi_u(s) = \mathcal{M}(p_u)(s) = \int_0^{+\infty} p_u(u) u^{s-1} du, \quad s \in \mathbb{C}.$$

The derivatives  $\kappa_\nu = [\ln \phi_u]^{(\nu)}(1)$  are the  $\nu$ th-order log-cumulants, where  $^{(\nu)}$  stands for the  $\nu$ th derivative,  $\nu = 1, 2, \dots$ . In case of the transform convergence, the following MoLC equations take place [2]

$$\begin{cases} \kappa_1 = E\{\ln u\} \\ \kappa_j = E\{(\ln u - \kappa_1)^j\}, \quad j = 2, 3. \end{cases}$$

Analytically expressing  $\kappa_j$  as functions of the unknown parameters and estimating these log-cumulants in terms of sample log-moments, one derives a system of nonlinear equations. These equations have one solution for any observed values of the log-cumulants for all the pdfs in  $\mathcal{D}$  (see Table I), except for, in some cases, the GGR,  $\mathcal{K}$ -root (see [10]), and GFD due to a complicated parameter estimation procedure.

For the purpose of the  $K$  estimation, [10] suggested running the DSEM for all values of  $K$  from 1 to a predefined  $K_{\max}$  and then choosing the number  $K^*$  that provides the highest log-likelihood estimate. In this letter, in order to avoid this computationally costly procedure, we adopt a  $K$  estimation procedure similar to the one suggested in [11] that consists of initializing the SEM with  $K_0 = K_{\max}$  and then allowing the components to be eliminated from the mixture during the iterative process once their priors  $P_i$  become too small, thus decreasing  $K$ . This strategy provides fast  $K^*$  estimates consistent with the DSEM estimates, allowing to reduce significantly the DSEM computation complexity, particularly for the high values of  $K_{\max}$ .

Thus, each iteration of the EDSEM goes as enumerated:

- 1) **E-step:** Compute, for each greylevel  $z$  and  $i$ th component, the posterior probability estimates corresponding to the current pdf estimates, i.e.,  $z = 0, \dots, Z - 1$

$$\tau_i^t(z) = \frac{P_i^t p_i^t(z)}{\sum_{j=1}^{K_t} P_j^t p_j^t(z)}, \quad i = 1, \dots, K_t$$

where  $p_i^t(\cdot)$  is the  $\sigma_i$ -conditional pdf estimate on the  $t$ th step.

- 2) **S-step:** Sample the label  $s^t(z)$  of each greylevel  $z$  according to the current estimated posterior probability distribution  $\{\tau_i^t(z) : i = 1, \dots, K_t\}$ ,  $z = 0, \dots, Z - 1$ .
- 3) **MoLC-step:** For the  $i$ th mixture component, compute the following histogram-based estimates of the mixture

proportions and the first three log-cumulants

$$P_i^{t+1} = \frac{\sum_{z \in Q_{it}} h(z)}{\sum_{z=0}^{Z-1} h(z)} \quad \kappa_{1i}^t = \frac{\sum_{z \in Q_{it}} h(z) \ln z}{\sum_{z \in Q_{it}} h(z)}$$

$$\kappa_{bi}^t = \frac{\sum_{z \in Q_{it}} h(z) (\ln z - \kappa_{1i}^t)^b}{\sum_{z \in Q_{it}} h(z)}, \quad i = 1, \dots, K_t$$

where  $b = 2, 3$ ,  $h(z)$  is the image histogram, and  $Q_{it} = \{z : s^t(z) = \sigma_i\}$  is the set of grey levels assigned to the  $i$ th component. Then, solve the corresponding MoLC equations (see Table I) for each parametric family  $f_j(\cdot|\theta_j)$  ( $\theta_j \in A_j$ ) in the dictionary, thus computing the resulting MoLC estimate  $\theta_{ij}^t$ ,  $j = 1, \dots, M$ .

- 4) **K-step:**  $\forall i$ ,  $i = 1, \dots, K_t$ . If  $P_i^{t+1} < \gamma$ , eliminate the  $i$ th component and update  $K_{t+1}$ . The choice of threshold  $\gamma$  does not appreciably affect the EDSEM provided that it is small, e.g., 0.005.
- 5) **Model-step:** For each mixture component  $i$ , compute the log-likelihood of each estimated pdf  $f_j(\cdot|\theta_{ij}^t)$  according to the data assigned to the  $i$ th component

$$L_{ij}^t = \sum_{z \in Q_{it}} h(z) \ln f_j(z|\theta_{ij}^t), \quad i = 1, \dots, K_{t+1}$$

and define  $p_i^{t+1}(\cdot)$  as the estimated pdf  $f_j(\cdot|\theta_{ij}^t)$  yielding the highest value of  $L_{ij}^t$ ,  $j = 1, \dots, M$ .

The sequence of estimates  $\Theta_t$  generated by the SEM converges to a unique stationary distribution, and the maximum likelihood estimate of the mixture parameters is asymptotically equivalent to the mathematical expectation of this stationary distribution. This behavior has been proved under suitable assumptions [11], which do not hold strictly for all the pdfs in  $\mathcal{D}$ . However, we recall that the SEM, compared to the classical EM or other deterministic variants for the FMM, was specifically designed to improve the exploratory properties of the EM in case of a multimodal likelihood function [11].

### III. EXPERIMENTAL RESULTS

#### A. Data Sets for Experiments

The EDSEM was tested on the following VHR SAR data sets:

- Single-look COSMO-SkyMed, Stripmap, approximately 2.5-m ground resolution, HH-polarized image acquired over Piemonte, Italy (Italian Space Agency (ASI), 2008). We present the experiments with two portions, CSK1 and CSK2 (see Fig. 1).
- Single-look image, acquired by the RAMSES airborne sensor, approximately 0.5-m resolution, acquired over Toulouse, France (Centre National d'Etudes Spatiales (CNES), 2004), hereafter denoted as RAMS (see Fig. 1).
- Two-look TerraSAR-X, Stripmap, approximately 6-m resolution, HH-polarized image acquired over Sanchangang, China (Infoterra, 2008). We present the experiments with two portions, TSX1 and TSX2 (see Fig. 2).
- Single-look TerraSAR-X, HR Spotlight, approximately 1-m resolution, VV-polarized image acquired over Barkedji, Senegal (CNES, 2007), denoted as TSXH (see Fig. 2).



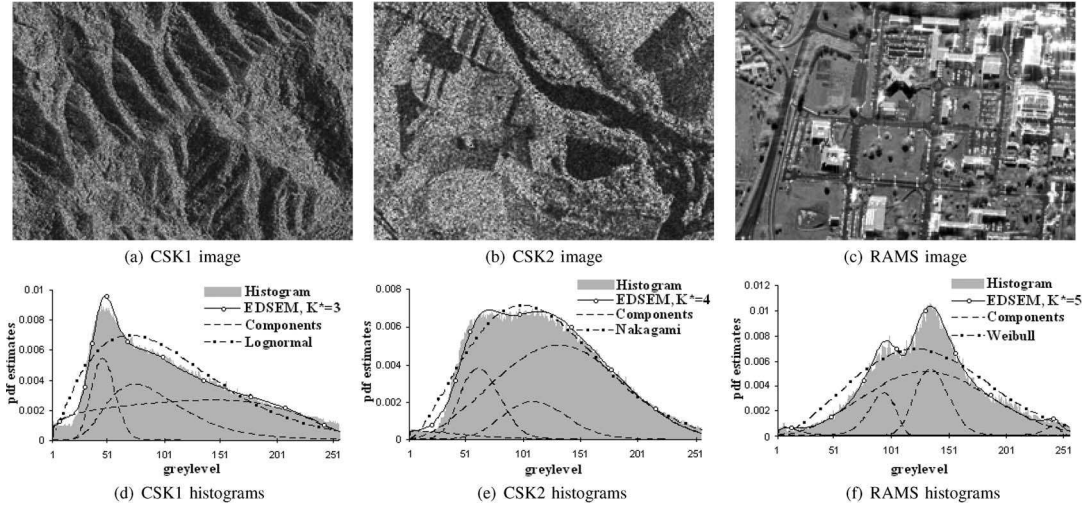


Fig. 1. (a) CSK1, (b) CSK2, and (c) RAMS images with (d)–(f) corresponding plots of pdf estimates. The plots contain the normalized image histograms, the EDSEM pdf estimates with the plots of  $K^*$  components in the estimated mixture, and the plots of the best fitting pdf models from  $\mathcal{D}$ .

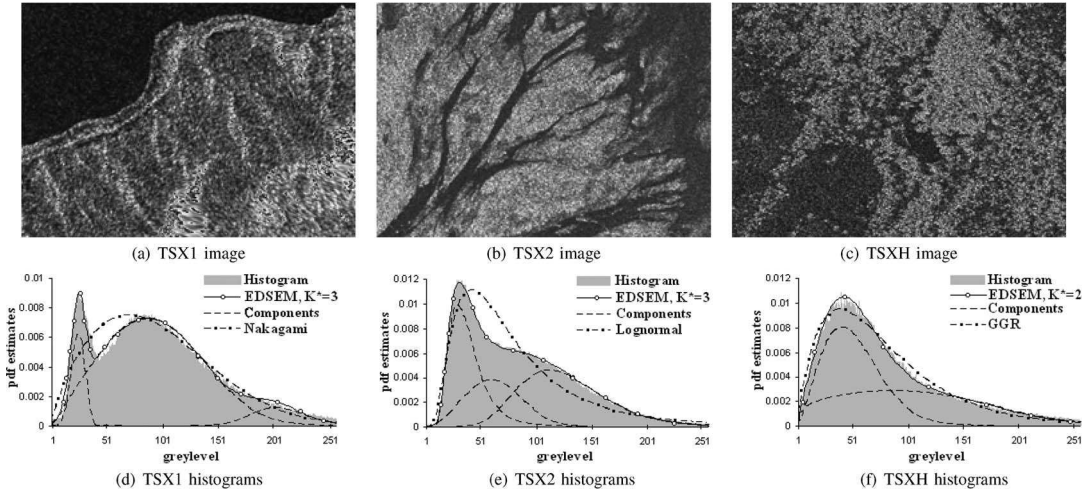


Fig. 2. (a) TSX1, (b) TSX2, and (c) TSXH images with (d)–(f) corresponding plots of pdf estimates. The plots contain the normalized image histograms, the EDSEM pdf estimates with the plots of  $K^*$  components in the estimated mixture, and the plots of the best fitting pdf models from  $\mathcal{D}$ .

All the employed images present heterogeneous scenes and, except for CSK2 and TSXH, exhibit multimodal histograms. The size of all the test images is 500 pixels  $\times$  500 pixels.

### B. PDF-Estimation Results

The obtained EDSEM pdf estimates have been assessed quantitatively by computing the Kolmogorov–Smirnov distances ( $\mathcal{K}\mathcal{S}$ ) between the estimates and normalized image histograms. The estimates were also assessed by the Kolmogorov–Smirnov goodness-of-fit test [13], and the corresponding  $p$ -values are reported in Table II. Here,  $p$  can be interpreted as a confidence level at which the corresponding fit hypothesis will be rejected. The following EDSEM parameters were used: the initial number of mixture components  $K_0 = 6$  and the number of iterations  $T = 200$ . Both were set manually high enough to give a sufficient burn-in for the SEM, and their further increase did not affect the results. For comparison, for all the images, we provide the best fitting pdf (with the smallest  $\mathcal{K}\mathcal{S}$ ), with the parameters estimated by the MoLC, among the eight models in  $\mathcal{D}$  (see Table II). For the considered

TABLE II  
EDSEM RESULTS:  $K^*$  ESTIMATE, THE ESTIMATED MIXTURE ( $f_i$ 'S AS IN TABLE I), KOLMOGOROV–SMIRNOV DISTANCE  $\mathcal{K}\mathcal{S}$ ,  $p$ -VALUE FOR THE KOLMOGOROV–SMIRNOV TEST, THE COMPUTATION TIME  $t$  (IN SECONDS), ALONG WITH THE BEST FITTING MODEL IN  $\mathcal{D}$  WITH  $\mathcal{K}\mathcal{S}$  AND  $p$ -VALUE

| Image | EDSEM estimate |                           |                          |            | Best fit in $\mathcal{D}$ |       |                          |            |
|-------|----------------|---------------------------|--------------------------|------------|---------------------------|-------|--------------------------|------------|
|       | $K^*$          | Mixture                   | $\mathcal{K}\mathcal{S}$ | $p$ -value | $t$                       | Model | $\mathcal{K}\mathcal{S}$ | $p$ -value |
| CSK1  | 3              | $f_4, f_4, f_5$           | 0.011                    | 0.9989     | 121s                      | $f_1$ | 0.062                    | 0.2787     |
| CSK2  | 4              | $f_5, f_4, f_1, f_5$      | 0.007                    | 1.0        | 192s                      | $f_5$ | 0.020                    | 0.9869     |
| RAMS  | 5              | $f_4, f_2, f_1, f_2, f_2$ | 0.008                    | 1.0        | 253s                      | $f_2$ | 0.059                    | 0.3349     |
| TSX1  | 3              | $f_2, f_1, f_7$           | 0.006                    | 1.0        | 155s                      | $f_5$ | 0.037                    | 0.8747     |
| TSX2  | 3              | $f_4, f_3, f_2$           | 0.004                    | 1.0        | 148s                      | $f_1$ | 0.058                    | 0.3552     |
| TSXH  | 2              | $f_6, f_4$                | 0.008                    | 1.0        | 97s                       | $f_7$ | 0.016                    | 0.9936     |

images, the accuracy improvement granted by the EDSEM is significant ( $\Delta\mathcal{K}\mathcal{S}$  up to 0.05) and somewhat smaller for the almost unimodal histograms (CSK2 and TSXH). The visual analysis of the EDSEM estimate plots (see Figs. 1 and 2) confirms an important improvement in the estimation accuracy.

The computation time of the EDSEM is presented in Table II, and the experiments were conducted on an Intel Core 2 Duo 1.83-GHz 1-Gb RAM, Windows XP system. Compared to the

TABLE III

NUMBERS OF TIMES THE MODELS IN  $\mathcal{D}$  WERE CHOSEN FOR MIXTURE COMPONENTS DURING EDSEM FOR CSK1, RAMS, AND TSXH IMAGES

| Image | $f_1$ | $f_2$ | $f_3$     | $f_4$ | $f_5$ | $f_6$     | $f_7$ | $f_8$     | Total |
|-------|-------|-------|-----------|-------|-------|-----------|-------|-----------|-------|
| CSK1  | 192   | 155   | <b>47</b> | 209   | 194   | <b>9</b>  | 53    | <b>25</b> | 793   |
| RAMS  | 145   | 265   | <b>7</b>  | 340   | 172   | <b>13</b> | 94    | <b>10</b> | 1046  |
| TSXH  | 45    | 69    | <b>5</b>  | 224   | 107   | <b>36</b> | 61    | <b>17</b> | 564   |

DSEM, the EDSEM allowed the following improvements: It worked 3.85 times faster for CSK1, 2.63 for RAMS, and 5.88 for TSXH (with the same  $K_{\max}$  and  $T$ ). We stress here the consistency of the results reported by both techniques in terms of  $K^*$ ,  $\mathcal{KS}$ , and  $p$ -value.

Finally, we address the issue of the dictionary content. We would like to mention that, given a new model not contained in  $\mathcal{D}$  provided with the corresponding MoLC equations and solution, the process of adding this model into the dictionary is straightforward. We study the number of times the pdfs in  $\mathcal{D}$  were chosen in the **Model-step** for mixture components along the EDSEM process (see Table III). The least frequently chosen models (in bold) were the Fisher,  $\mathcal{K}$ -root, and  $S\alpha SGR$ . Additional experiments with a dictionary of five models (without  $f_3$ ,  $f_6$ , and  $f_8$ ) reported a negligible decline in the accuracy (a  $\mathcal{KS}$  increase of less than 0.005), suggesting a smaller significance of these models in  $\mathcal{D}$ . The computational speedup, however, was significant due to the cumbersome numerical procedures for the  $\mathcal{K}$ -root and  $S\alpha SGR$ . A further refinement of  $\mathcal{D}$  can be achieved by removing the Weibull pdf which is a particular case of the GFD. Thus, very accurate results can be achieved with dictionary  $\hat{\mathcal{D}} = \{f_1, f_4, f_5, f_7\}$ : The same estimate was obtained for CSK1 in 78 s; compared to the result in Table II,  $f_2$  was replaced by  $f_4$  in the estimate for RAMS, which achieved  $\mathcal{KS} = 0.01$  and took 157 s; similarly,  $f_6$  was replaced by  $f_5$  in the estimate for TSXH with  $\mathcal{KS} = 0.012$  and 62 s. Thus, this dictionary refinement further reduces the computation time of the EDSEM by 35% on the average, only marginally affecting the accuracy (the increase in  $\mathcal{KS}$  is always below 0.007).

#### IV. CONCLUSION

In this letter, we have proposed a general flexible pdf-estimation method for the SAR images and specifically validated it on the heterogeneous VHR SAR data, which represent a very current and relevant case in which the heterogeneous behavior is expected. The developed model is based on the DSEM approach recently developed in [10] for a medium-resolution SAR. The extension of the proposed method to the intensity data (instead of amplitudes) is straightforward, which is done by replacing the amplitude pdfs in the dictionary with the corresponding intensity pdfs.

The contribution of this letter is twofold. First, the developed EDSEM algorithm extends DSEM to the novel type of imagery (heterogeneous VHR) and is enhanced by a novel efficient procedure for estimating the number of mixture components. It reported very accurate and computationally fast estimation results in the experiments with the VHR SAR images acquired by the modern satellite systems TerraSAR-X and COSMO-SkyMed, and RAMSES airborne sensor. We stress here that the problem of modeling the statistics of the VHR satellite SAR amplitude images has not been addressed so far, and the proposed EDSEM technique looks very promising for this

type of images, since it is based on a finite mixture approach and intrinsically takes into account the heterogeneity, which is an inherent VHR image property. Second, we studied the extended dictionary of the SAR-specific pdfs (including the Fisher and GFD models) and analyzed the refinement options. This study have suggested that, at least on the considered data sets, the dictionary reduction from eight to four models affects the estimation accuracy only marginally, on the other hand permitting to reduce the computation burden of the EDSEM by 35%.

The reported results have suggested the EDSEM to be an attractive approach for various application problems, e.g., it can be efficiently used for SAR image segmentation (to discriminate the resulting mixture components) [10] and for class-conditional pdf modeling in the supervised VHR SAR classification [14].

#### ACKNOWLEDGMENT

This research has been conducted within a collaboration between the Institut National de Recherche en Informatique et en Automatique (INRIA) Sophia Antipolis, France, and the Department of Biophysical and Electronic Engineering (DIBE), University of Genoa, Italy. The authors would like to thank the ASI for providing the employed COSMO-SkyMed image and the CNES for providing the RAMSES and the TerraSAR-X Barkedji images. The TerraSAR-X image of Sanchagang was taken from <http://www.infoterra.de/>.

#### REFERENCES

- [1] C. Oliver and S. Quegan, *Understanding Synthetic Aperture Radar Images*. Norwood, MA: Artech House, 1998.
- [2] C. Tison, J.-M. Nicolas, F. Tupin, and H. Maitre, "A new statistical model for Markovian classification of urban areas in high-resolution SAR images," *IEEE Trans. Geosci. Remote Sens.*, vol. 42, no. 10, pp. 2046–2057, Oct. 2004.
- [3] R. O. Duda, P. E. Hart, and D. G. Stork, *Pattern Classification*. New York: Wiley-Interscience, 2001.
- [4] P. Mantero, G. Moser, and S. B. Serpico, "Partially supervised classification of remote sensing images using SVM-based probability density estimation," *IEEE Trans. Geosci. Remote Sens.*, vol. 43, no. 3, pp. 559–570, Mar. 2005.
- [5] H.-C. Li, W. Hong, and Y.-R. Wu, "Generalized Gamma distribution with MoLC estimation for statistical modeling of SAR images," in *Proc. APSAR*, Huangshan, China, 2007, pp. 525–528.
- [6] G. Moser, J. Zerubia, and S. B. Serpico, "SAR amplitude probability density function estimation based on a generalized Gaussian model," *IEEE Trans. Image Process.*, vol. 15, no. 6, pp. 1429–1442, Jun. 2006.
- [7] E. E. Kuruoglu and J. Zerubia, "Modelling SAR images with a generalization of the Rayleigh distribution," *IEEE Trans. Image Process.*, vol. 13, no. 4, pp. 527–533, Apr. 2004.
- [8] E. Jakeman and P. N. Pusey, "A model for non-Rayleigh sea echo," *IEEE Trans. Antennas Propag.*, vol. AP-24, no. 6, pp. 806–814, Nov. 1976.
- [9] A. C. Frery, H.-J. Muller, C. C. F. Yanasse, and S. Sant'Anna, "A model for extremely heterogeneous clutter," *IEEE Trans. Geosci. Remote Sens.*, vol. 35, no. 3, pp. 648–659, May 1997.
- [10] G. Moser, S. B. Serpico, and J. Zerubia, "Dictionary-based stochastic expectation maximization for SAR amplitude probability density function estimation," *IEEE Trans. Geosci. Remote Sens.*, vol. 44, no. 1, pp. 188–200, Jan. 2006.
- [11] G. Celeux, D. Chauveau, and J. Diebolt, "On stochastic versions of the EM algorithm," INRIA, France, Res. Rep. 2514, 1995.
- [12] I. Sneddon, *The Use of Integral Transforms*. New York: McGraw-Hill, 1972.
- [13] M. Stephens, "Test of fit for the logistic distribution based on the empirical distribution function," *Biometrika*, vol. 66, no. 3, pp. 591–595, Dec. 1979.
- [14] G. Moser, V. Krylov, S. B. Serpico, and J. Zerubia, "High resolution SAR-image classification by Markov random fields and finite mixtures," in *Proc. SPIE*, San Jose, CA, 2010, vol. 7533, pp. 753308-01–753308-12.